Pergamon

Int. J. Heat Mass Transfer. Vol. 41, No. 15, pp. 2279–2285, 1998

Printed in Great Britain
0017–9310/98 $19.00 + 0.00

PII: S0017–9310(97)00359–1

Applicability of photothermal radiometry for temperature measurement of semiconductors

G. CHEN† and T. BORCA-TASCIUC

Mechanical and Aerospace Engineering Department, University of California at Los Angeles, Los Angeles, CA 90095-1597, U.S.A.

(*Received* 17 *July* 1997 *and in final form* 7 *November* 1997)

Abstract—This work explores the applicability of photothermal radiometry for the temperature measurement of semiconductors. Although this technique has been used to measure the surface temperature of metals, additional considerations must be given for temperature measurement of semiconductors due to electron-hole pair generation by the laser. Criteria for the applicability of photothermal radiometry to temperature measurement of semiconductors are established in this work and experimental results are presented for temperature measurement of a silicon sample in a radiation environment. This study demonstrates that photothermal radiometry can be applied to the temperature measurement of heavily-doped samples, but care must be taken to minimize the effect of electron-hole pair generation by choosing appropriate experimental conditions.

INTRODUCTION

Radiation thermometry has been widely employed for temperature measurement in various industrial processes [1]. There exist, however, two factors limiting the accuracy of radiation thermometry. One is related to the unknown emissivity of the sample and the other is the influence of the ambient radiation. The first issue, although still remains challenging, has been addressed extensively in the literature. Various emissivity correction methods such as *in situ* emissivity characterization [2], two-color, and multi-color pyrometry have been developed [1, 3]. The second issue has also been treated, mostly by improving the optical system to reduce the ambient radiation reaching the detector. Although those developments have greatly improved the accuracy and extended the application of radiation radiometry, there are still many industrial processes that require radiation radiometry with better accuracy.

An alternative approach to minimize the ambient radiation effect is based on a photothermal effect [4] that is created by an external laser source. The sample temperature change can generate various detectable signals such as surface reflectivity, acoustic and thermal waves, and thermal emission. Experimental techniques based on the detection and analysis of the photothermal emission signal from the sample have been employed in numerous applications including thermophysical and electronic property characterization, nondestructive testing, and optical spectroscopy, and they are often called photothermal radiometry in these applications [5, 6]. The use of photothermal effect for direct temperature has been explored by Loarer and co-workers [7, 8] on stainless steel samples heated inside a furnace, and by Eyal *et al.* [9] on a blackbody source. Markham *et al.* [10] combined such a photothermal effect with a spectrometer to develop an emissivity independent temperature measurement technique for monitoring combustion process. The temperature perturbation in these experiments can be periodic [7, 10] or stepwise [8, 9]. The advantage of temperature modulation is that the relatively weak photothermal signal can be captured easily with a lock-in amplifier. The advantage of a stepwise temperature perturbation is that fast processes can be monitored.

The application of the photothermal radiometry technique to semiconductor sample temperature measurement is more problematic because of electron-hole pair generation when the excitation photon energy is larger than the bandgap of the semiconductor. The generated electrons and holes contribute to the thermal emission signal by changing the radiative properties of the sample. Such an electronic effect has been utilized for nondestructive diagnosis of electronic properties such as dopant concentration, electronic diffusivity, and recombination time [6].

This work explores the potential of photothermal radiometry for temperature monitoring in semiconductor manufacturing processes. Conditions for successful temperature measurement of semiconductor samples by the photothermal radiometry method will first be established based on an order

† Author to whom correspondence should be addressed. Tel.: 001 310 206 7044. Fax: 001 310 206 2302. E-mail: gchen@seas.ucla.edu.

NOMENCLATURE

A	area [m^2]
B	detector responsivity [A/W]
c	volumetric specific heat [J cm^{-3} K^{-1}]
C	system constant [A · μm]
D	diffusivity [cm^2 s^{-1}]
E	emissive power [W m^{-2}]
f	frequency [Hz]
F	view factor
G	signal ratio
h	Planck constant [J s]
k	thermal conductivity [W cm^{-1} K^{-1}]
K	system constant
l	diffusion length [cm]
L	thickness of semiconductor wafer [cm]
n	carrier density [cm^{-3}]
P	absorbed power [W]
r_0	radius of laser beam [cm]
R	reflectivity at air–semiconductor interface
S	signal [A]
t	time [s]
T	temperature [K]
V	volume [cm^3].

Greek symbols

α_λ	absorption coefficient [cm^{-1}]
$\Delta\lambda$	bandwidth [μm]
ε	emissivity
λ	signal wavelength [μm]
ν	laser photon frequency [Hz]
ρ	reflectivity
τ	transmissivity
ω	angular frequency [Hz].

Subscripts

a	ambient
ac	modulated
b	blackbody
dc	unmodulated
e	electronic
L	laser
0	unperturbed
s	sample
t	thermal
λ	wavelength.

of magnitude analysis, followed by a presentation of experimental results on the temperature measurement of a silicon sample inside a furnace.

ORDER OF MAGNITUDE ANALYSIS

The principle of photothermal radiometry has been presented in the work of Loarer *et al.* [7, 8]. The basic idea is to create a small perturbation in the sample temperature using an external laser source. This small temperature perturbation is superimposed on the original sample temperature and creates a corresponding change in the thermal emission signal from the sample. Instead of measuring the direct thermal emission from the sample, the perturbed thermal emission signal is detected and used to obtain the absolute temperature of the sample. Under appropriate conditions [7], the perturbed signal is not affected by the ambient radiation.

Electron-hole pairs may be generated inside semiconductor wafers if the laser used to create the temperature perturbation has a wavelength shorter than that corresponding to the semiconductor bandgap. These electron-hole pairs participate in the thermal emission and thus affect the accuracy of the temperature measurement. Although studies have been reported on the effect of electron-hole pair generation on the photothermal emission and photothermal reflection signals based on solving the coupled carrier diffusion and heat conduction equations [11–13], no simple analytical rules have been proposed to guide the selection of experimental conditions such that the effect of electron-hole pair generation is minimized. In this section, criteria for successful temperature measurement of semiconductors by the photothermal radiometry method will be established based on an order of magnitude analysis.

For a system as shown in Fig. 1, the signal generated in the radiation detector is

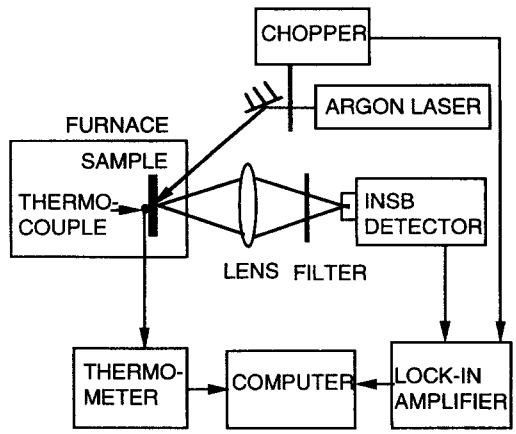

Fig. 1. Schematic drawing of a photothermal radiometry system for temperature measurement of a sample in a furnace.

$$S_\lambda = C_\lambda \int_A \{\varepsilon_{s\lambda} E_{b\lambda}(T) + \varepsilon_{f\lambda}[\rho_{s\lambda} F_{sff} + \tau_{s\lambda} F_{sfb}] E_{b\lambda}(T_a)\}\, dA \quad (1)$$

where C_λ ($=\tau_{0\lambda} F_{sd} B_\lambda \Delta\lambda$) is a system constant depending on wavelength (λ) and bandwidth ($\Delta\lambda$), the detector responsivity (B_λ), and the optical transmissivitity ($\tau_{0\lambda}$) from the sample to the detector. The integration in equation (1) is over the area that can be viewed by the detector. The first term inside the bracket is the product of the sample emissivity ($\varepsilon_{s\lambda}$) and its blackbody radiative power ($E_{b\lambda}$). The last two terms represent the ambient radiation, denoted by a temperature T_a and the ambient emissivity $\varepsilon_{f\lambda}$, reaching the detector through the sample reflection (as represented by reflectivity $\rho_{s\lambda}$) and transmission (as represented by transmissivity $\tau_{s\lambda}$). The geometrical view factors from the front and back of the sample to the ambient are denoted by F_{sff} and F_{sfb}, respectively.

Photothermal radiometry reduces the effect of the ambient radiation by introducing a small perturbation in the sample temperature and measures the perturbed signal. If the radiative properties of the sample are independent of its temperature, the last two terms do not appear in the perturbed signal, which means a total elimination of the ambient effect. Because radiative properties generally depend on temperature, the ambient radiation contributes to the perturbed signal through the perturbation of the reflectivity and transmissivity of the sample. To minimize the ambient effect, the temperature dependence of the radiative properties of the target should be small [14]. This requirement means that the photothermal radiometry technique is not applicable to lightly-doped silicon samples from 300–900 K where their emissivities depend strongly on temperature. With this in mind, the following discussion will no longer include the ambient effect but focus on the effect of electron-hole pair generation on the perturbed signal, i.e., the last two terms in equation (1) will be dropped such that

$$S_\lambda = C_\lambda \int_A \varepsilon_{s\lambda} E_{b\lambda}(T)\, dA. \quad (2)$$

The temperature perturbation considered in this work is created by a modulated external laser beam. The temperature in the vicinity of the irradiated area becomes

$$T(r) = T_0 + T_{dc}(r) + T_{ac}(r)\, e^{i\omega t} \quad (3)$$

where T_0 is the original sample temperature, T_{dc} the d.c. temperature rise caused by the laser heating, and T_{ac} the amplitude of the sample temperature oscillation. In addition to the temperature perturbation, the laser also creates electron-hole pairs if its photon energy is larger than the bandgap. The local electron-hole pair density consists of three terms similar to the temperature distribution,

$$n(r) = n_0 + n_{dc}(r) + n_{ac}(r)\, e^{i\omega t} \quad (4)$$

where n_0 is the intrinsic carrier concentration at temperature T_0, n_{dc} the d.c. carrier distribution and n_{ac} the amplitude of the carrier concentration oscillation. In addition to direct electron-hole generation by the laser beam, the carrier concentration is also dependent on the local temperature due to band gap variation with temperature. The effect of temperature variation on the last two terms in equation (4) is small compared to direct electron-hole generation by the laser beam.

The modulation in temperature and carrier density creates a modulation in the detected signal. While the blackbody emissive power depends only on temperature, emissivity of semiconductors depends on both temperature and the carrier density. Substituting equations (3) and (4) into equation (2) and using Taylor expansion yields the a.c. component of the signal as

$$S_{\lambda ac} = C_\lambda \int_A \left\{ \frac{\partial \varepsilon_{s\lambda}}{\partial T} T_{ac} E_{b\lambda} + \frac{\partial \varepsilon_{s\lambda}}{\partial n} n_{ac} E_{b\lambda} + \varepsilon_{s\lambda} \frac{\partial E_{b\lambda}}{\partial T} T_{ac} \right\} dA \quad (5)$$

where the values of emissivity, the blackbody emissive power, and their derivatives are taken at $T_0 + T_{dc}$ and $n_0 + n_{dc}$. It is assumed that the d.c. temperature rise can be calibrated and the sample temperature to be discussed later refers to $T_0 + T_{dc}$.

To accurately determine the sample temperature based on the measured ac signals, the first two terms in equation (5) must be much smaller than the last term, i.e., the signal is dominated by the modulation in the emissive power. This leads to the requirement that the dependencies of emissivity on temperature and carrier concentration must be small. A more quantitative discussion on the requirement of the temperature dependence of emissivity has been given before in conjunction with the elimination of the ambient effect [7, 14]. The emphasis here will be on establishing conditions such that the electron-hole pair generation effect can be minimized. This requires

$$\int_A \frac{\partial \varepsilon_{s\lambda}}{\partial n} n_{ac} E_{b\lambda}\, dA \ll \int_A \varepsilon_{s\lambda} \frac{\partial E_{b\lambda}}{\partial T} T_{ac}\, dA. \quad (6)$$

The above integration depends on the actual distributions of the a.c. temperature and carrier concentration, which could be obtained from solving the carrier and the thermal diffusion equations [11–13]. The solutions are complicated due to coupling of the two equations. The following order of magnitude analysis will lead to a simple criterion that can be used to guide the design of experiment.

Order of magnitude speaking, equation (6) can be expressed as

$$\frac{\partial \varepsilon_{s\lambda}}{\partial n} n_{ac} E_{b\lambda} A_{eac} \ll \varepsilon_{s\lambda} \frac{\partial E_{b\lambda}}{\partial T} T_{ac} A_{tac} \quad (7)$$

where A_{eac} and A_{tac} are the a.c. affected region due to

electron-hole pair modulation and temperature modulation, respectively; n_{ac} and T_{ac} are the characteristic amplitudes of carrier and temperature modulation, respectively. In taking the a.c. affected area rather than the detector viewed area, it is implied that the a.c. affected area is smaller than the detector viewed area.

The a.c. affected area is proportional to

$$A_{ac} \sim \pi(r_0 + l_{ac})^2 \tag{8}$$

where l_{ac} is the diffusion length (electronic or thermal) and r_0 is the radius of the laser beam. The diffusion length is proportional to the square root of the product of the (electronic or thermal) diffusivity and a characteristic time.

The ac diffusion of electron-hole pairs is determined by the shorter of two characteristic times: the recombination time and the modulation period. As it will become clear later, the modulation period must be long. The electronic diffusion length thus is determined by the recombination time, $l_{eac} \sim \sqrt{D_e \tau}$, where D_e is the electron-hole pair diffusivity and τ the recombination time. At room temperature, electron-hole pair diffusivity is $\sim 10\ \mathrm{cm^2\ s^{-1}}$ and the recombination time is typically less than 10^{-5} s [15], which leads to an electronic diffusion length less than $\sim 100\ \mu$m.

To determine the a.c. temperature response area, there are also two characteristic lengths to consider. One is the electronic diffusion length, which determines the size of the heat generation region because most of the energy released in the recombination process is converted into heat. The other is the thermal diffusion length: $l_{tac} \sim \sqrt{D_t/\omega}$, where ω is the angular modulation frequency. The thermal diffusivity, D_t, of silicon is $\sim 0.9\ \mathrm{cm^2\ s^{-1}}$ at room temperature. For a modulation frequency of 1 KHz, the thermal diffusion length is $\sim 120\ \mu$m. Since the modulation frequency must be low, the thermal diffusion length should be used in the evaluation of the a.c. temperature response area.

To estimate the amplitude of the modulation of the carrier concentration and temperature, a lumped analysis is used by assuming that all the excited electron-hole pairs are uniformly distributed in a volume determined by $V_{eac} = A_{eac} l_{eac}$, and that the heat generation is uniformly distributed inside a volume determined by $V_{tac} = A_{tac} l_{tac}$. The carrier generation density and temperature rise are then given by

$$n_{ac} \sim \frac{P\tau}{h\nu_L V_{eac}} \tag{9}$$

$$T_{ac} \sim \frac{P}{c\omega V_{tac}} \tag{10}$$

where h is the Planck constant, P the absorbed laser power, c the volumetric specific heat, and ν_L the frequency of the laser photon. Substituting equations (8)–(10) into equation (7) yields

$$\frac{\omega c \tau l_{tac}}{h\nu_L l_{eac} \varepsilon_{s\lambda}} \frac{\partial \varepsilon_{s\lambda}}{\partial n} \ll \frac{1}{E_{b\lambda}} \frac{\partial E_{b\lambda}}{\partial T}. \tag{11}$$

The normal emissivity of a semiconductor wafer can be expressed as

$$\varepsilon_\lambda = \frac{(1-R_\lambda)(1-e^{-\alpha_\lambda L})}{1-R_\lambda e^{-\alpha_\lambda L}} \tag{12}$$

where L is the wafer thickness, R_λ the reflectivity at air–semiconductor interface, and α_λ the absorption coefficient. The free-carrier density modulation can create variations in both the interface reflectivity and the absorption coefficient, and thus a modulation in the sample emissivity. The reflectivity variation as estimated from the Drude model is $\mathrm{d}R_\lambda/\mathrm{d}n \sim 10^{-22} R_\lambda$ [16]. The variation in the absorption coefficient can be estimated from an empirical relation between the absorption coefficient and free-carrier density as $\mathrm{d}\alpha_\lambda/\mathrm{d}n \sim 10^{-20} T\lambda^2\ (\mathrm{cm^2})$ [17], where wavelength λ is in micron. It can be shown that the modulation in the free-carrier density dominates the modulation of the sample emissivity, and that

$$\frac{\mathrm{d}\varepsilon_\lambda}{\mathrm{d}n} \approx (1-R_\lambda)^2 e^{-\alpha L_{l_{ac}}} \frac{\mathrm{d}\alpha_\lambda}{\mathrm{d}n}. \tag{13}$$

Combining equations (11)–(13) leads to the following criterion

$$\frac{10^{-20} c(1-R_\lambda) e^{-\alpha_\lambda L} \tau \sqrt{D_t \omega}}{h\nu} \ll \frac{C_2 e^{C_2/\lambda T}}{(\lambda T)^3 (e^{C_2/\lambda T} - 1)} \tag{14}$$

where C_2 ($= 14\,387\ \mu$m K) is a constant in the Planck distribution. For thermal radiation, the exponential term is very large and the above equation can be further simplified to

$$\sqrt{f} \ll \frac{1.15 \times 10^5 \sqrt{D_t}}{k\tau\lambda_L (\lambda T)^3 (1-R_\lambda) e^{-\alpha_\lambda L}} \tag{15}$$

where k is thermal conductivity in $\mathrm{W\ cm^{-1}\ K^{-1}}$, λ_L is the laser wavelength in micron. Using typical silicon properties at room temperature ($k = 1.42\ \mathrm{W\ cm^{-1}\ K^{-1}}$, $D_t = 0.9\ \mathrm{cm^2\ s^{-1}}$, $R_\lambda = 0.3$, $\tau = 10^{-5}$ s), and setting $e^{-\alpha_\lambda L} = 0.1$ and $\lambda_L = 0.5\ \mu$m yield $\sqrt{f} \ll 251\ \sqrt{\mathrm{Hz}}$ at room temperature. At high temperatures, for example at 900 K, the frequency limit is reduced by a factor of 27 if all the other quantities in equation (15) are temperature independent. In reality, thermal conductivity decreases and absorption coefficient increases with increasing temperature. Recombination time is also likely to decrease at high temperatures. These property variations increase the frequency limit and weaken the explicit inverse temperature dependence of the frequency limit in equation (15). For direct band gap semiconductors such as GaAs, the recombination time is much shorter ($\sim 10^{-9}$ s) and the modulation frequency can be higher.

If equation (15) is satisfied, the a.c. signal can be expressed as

$$S_{\lambda ac} = C_\lambda \varepsilon_{s\lambda} \frac{\partial E_{b\lambda}}{\partial T} T_{ac} A_{tac}. \quad (16)$$

The ratio of the a.c. signal at two different wavelengths can be used to eliminate the a.c. temperature rise and area,

$$G(T) = \frac{S_{\lambda_{1ac}}}{S_{\lambda_{2ac}}} = K \frac{\varepsilon_{s\lambda_1} \partial E_{b\lambda_1}/\partial T}{\varepsilon_{s\lambda_2} \partial E_{b\lambda_2}/\partial T} \quad (17)$$

where K represents the ratio of the products of the transmissivity of the optical system and the detector responsivity at the two wavelengths. The ratio of the sample emissivity at the two wavelengths runs into the classical problem in two-color pyrometry [1]. Often, wavelengths are chosen such that the emissivities are equal to each other. Another approach is to determine the emissivity of the sample through calibration. In the following work, the emissivities of the silicon sample will be assumed to equal each other for the chosen wavelengths.

EXPERIMENTAL RESULTS ON SILICON

Figure 1 shows the experimental system for implementing the photothermal pyrometry for measuring the surface temperature of a silicon sample situated in a furnace. The length of the tabular furnace is 15 cm and its inner diameter is 5 cm. A modulated argon laser is directed at the sample to create a small temperature modulation in the irradiated area. The bulk temperature of the sample is controlled by a furnace. The average sample temperature is measured by a K-type thermocouple with 127 μm diameter leads. Thermal emission of the sample from the irradiated area is collected by an infrared lens and detected by a liquid-nitrogen cooled InSb detector. The signal is sent to a lock-in amplifier and computer for data processing. A germanium window integrated into the detector blocks the argon beam scattered into the optical system. The wavelength of the thermal radiation is selected by two infrared filters centered at 3.205 μm and 4.51 μm, respectively. During the experiment, care is taken to avoid the heating of interference filters because their bandwidths are sensitive to temperature. The bandwidths of the filters are calculated from their transmission spectra provided by the manufacturer as 111 nm for the 3.205 μm filter and 65 nm for the 4.51 μm filter for an equivalent peak transmissivity of 100%. The signal at each wavelength is collected in separate runs.

Figure 2 shows the photothermal emission signals at two wavelengths for a heavily-doped n-type silicon sample with an electrical resistivity ~ 0.01 cmΩ. The corresponding carrier concentration in the silicon sample is $\sim 10^{17}$ cm^{-3} [15]. The laser power used is 166 mW and laser beam diameter is ~ 1.5 mm. The d.c. carrier concentration due to laser excitation is estimated to be $\sim 10^{16}$ cm^{-3} for a recombination time of 10^{-5} s. The d.c. temperature rise caused by the laser is about 3 K. The laser beam modulation is at 100 Hz.

The ratios of the two signals at 20 Hz and 100 Hz are shown in Fig. 3. To derive the temperature of the sample from the ratio of the photothermal signal at the two wavelengths, equation (17) is calculated based on the information on the filters and the detector

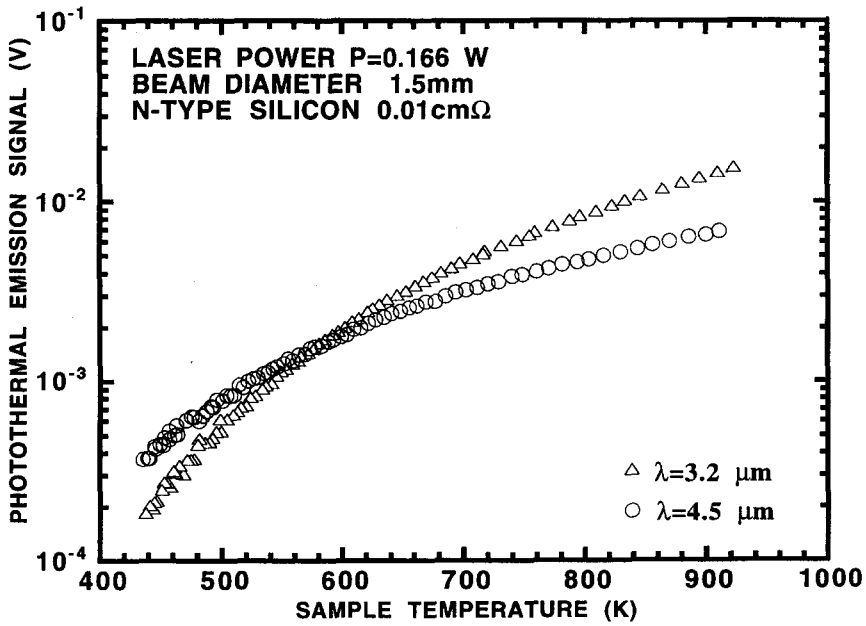

Fig. 2. Photothermal emission signals for a heavily doped silicon sample at two different wavelengths at 100 Hz.

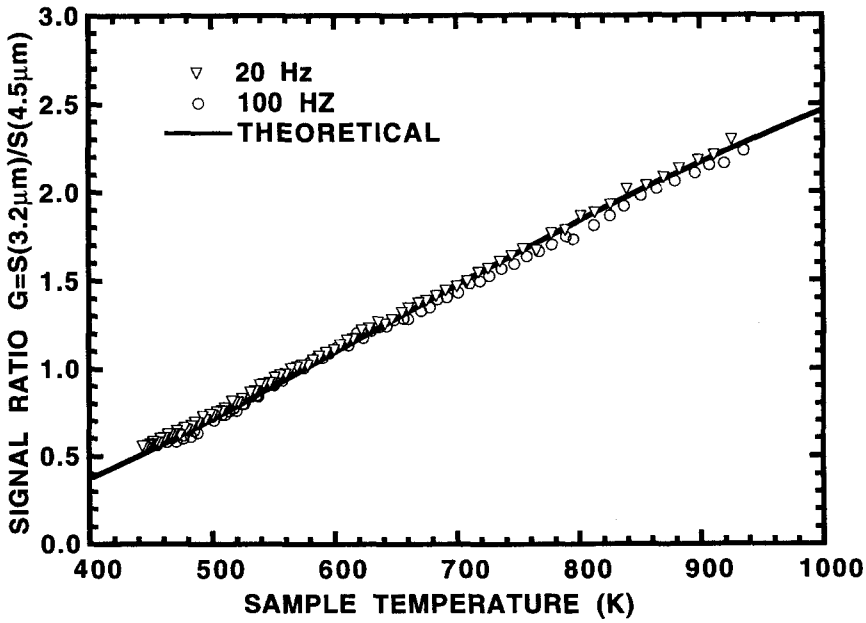

Fig. 3. Theoretical and experimental ratio of the photothermal emission signals for the silicon sample at 20 and 100 Hz.

provided by manufacturers and by assuming that the emissivities of the sample at the two wavelengths equal to each other. Although the emissivities of bare heavily-doped silicon wafers at 3.2 and 4.5 μm are close to each other [18], SiO_2 films developed on the surface can create interference effect and change the emissivity ratio. Theoretical calculations carried out based on wave optics show that the emissivity ratio is not changed from that of bare silicon samples for the oxide thickness in 20–500 Å range at the chosen wavelengths. The oxide growth rate at 700°C (the maximum experimental temperature) is <2.6 Å/h and the initial oxide thickness is ~ 20 Å. This slow oxidation rate is not expected to affect the results of the reported experiment. Calculated calibration curve according to equation (17) is shown in Fig. 3 as a solid line. The curve can be well represented by a cubic polynomial fit, which is used for deducing the sample temperature from the measured signal ratio.

A comparison of the thermocouple temperature reading and the corresponding photothermal radiometry temperature reading at a modulation frequency of 20, 100, and 500 Hz is shown in Fig. 4. An examination of the figure reveals that the experimental determination of the silicon sample temperature using the photothermal radiometry method is close to the thermocouple reading for the low temperature region. With increasing modulation frequency and at higher temperatures, the error tends to be larger, in qualitative agreement with equation (15). For 100 Hz, the maximum relative error between the radiometer and the thermocouple temperature reading is 3%. For 500 Hz modulation, the electronic effect is larger and the maximum relative error becomes 6.5% at 900 K. The experiment demonstrates that photothermal radiometry may be applied to heavily-doped semiconductor samples if the effect of electron-hole pairs can be minimized by careful consideration of experimental conditions. These conditions in turn limit the industrial process that can be monitored by the technique. For example, the slow modulation requirement makes it difficult to apply the technique to rapid thermal processes. It should be reminded, however, that the electron-hole generation can be avoided by choosing a laser with a wavelength longer than that corresponding to the semiconductor band gap.

CONCLUSIONS

This work explores the applicability of the photothermal radiometry technique for the temperature measurement of semiconductor samples. The effect of electron-hole pair generation due to the excitation laser beam is considered. Based on an order of magnitude analysis, criteria are established for successful temperature measurements of semiconductor samples by the photothermal radiometry method. Experimental results on a heavily doped silicon sample demonstrate the feasibility of photothermal radiometry as a tool for temperature measurement of heavily-doped semiconductors. The modulation frequency should be set at low value in these measurements to minimize the effect of electron-hole contribution to the photothermal emission signal.

Acknowledgement—This work is supported by a National Science Foundation Young Investigator Award to G.C.

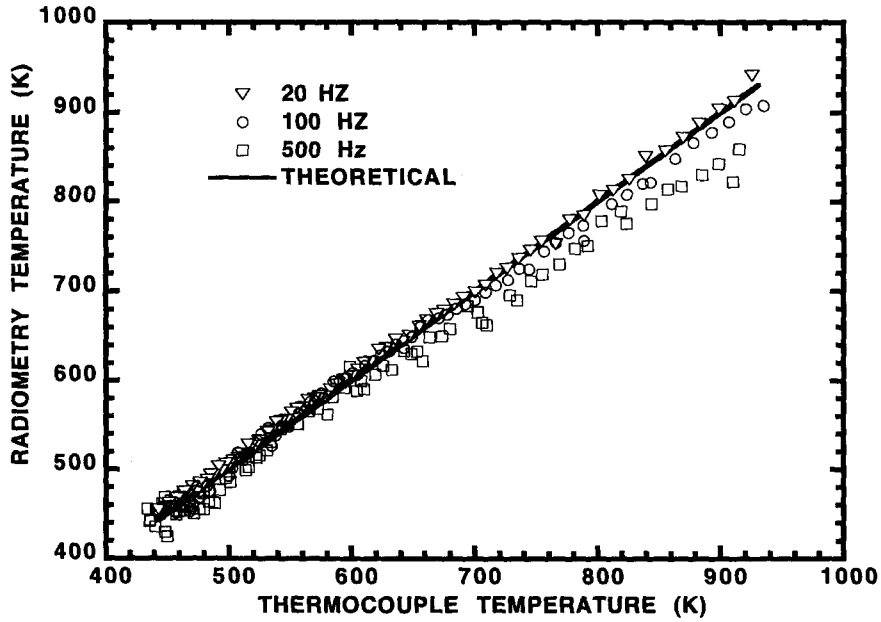

Fig. 4. Comparison of the thermocouple and photothermal radiometry temperature readings for the silicon sample at 20, 100 and 500 Hz.

REFERENCES

1. DeWitt, D. P. and Nutter, G. D., *Theory and Practice of Radiation Thermometry*. Wiley, New York, 1988.
2. Boebel, F. G., Moller, H., Wowchak, A., Hertl, B., Van Hove, J., Chow, L. A. and Chow, P. P., Pyrometric interferometry for real time molecular beam epitaxy process monitoring. *J. Vac. Sci. Tech. B*, 1994, **12**, 1207–1210.
3. DeWitt, D. P. and Kunz, H. Theory and technique for surface temperature determinations by measuring the radiance temperatures and the absorptance ratio for two wavelengths. In *Temperature: Its Measurement and Control in Science and Industry*, 1972, **4**, 599–610.
4. Berthet, O. and Greffet, J. J., Pyrometry using photothermal effect. *Proceedings of 8th International Heat Transfer Conference*. San Francisco, 1986, pp. 561–564.
5. Tam, A. C., Pulsed photothermal radiometry for noncontact spectroscopy, material testing and inspection measurements. *Infr. Phys.*, 1985, **25**, 305–313.
6. Mandelis, A., ed., *Photoacoustic and Thermal Wave Phenomena in Semiconductors*. North-Holland, New York, 1987.
7. Loarer, T., Greffet, J. J. and Heutz-Aubert, M., Noncontact surface temperature measurement by means of a modulated photothermal effects. *Appl. Opt.*, 1990, **29**, 979–987.
8. Loarer, T. and Greffet, J. J., Application of the pulsed photothermal effect to fast surface temperature measurements. *Appl. Opt.*, 1992, **31**, 5350–5358.
9. Eyal, O., Scharf, V. and Katzir, A., Temperature measurements using pulsed photothermal radiometry and silver halide infrared optical fibers. *Appl. Phys. Lett.*, 1997, **70**, 1509–1511.
10. Markham, J. R., Best, P. E. and Solomon, P. R., Spectroscopic method for measuring surface temperature that is independent of material emissivity, surrounding radiation sources, and instrument calibration. *Applied Spectroscopy*, 1994, **48**, 265–270.
11. Boccara, A. C. and Fournier, D., Thermal wave investigation of transport properties of semiconductors. I. Methodology. In *Photoacoustic and Thermal Wave Phenomena in Semiconductors*, ed. A. Mandelis. New York, North-Holland, 1987, pp. 287–310.
12. Sheard, S. J. and Somekh, M. G., Semiconductor assessment using photothermal radiometry. *Infr. Phys.*, 1988, **28**, 287–292.
13. Christofides, C., Diaknos, F., Seas, A., Christou, C., Nestoros, M. and Mandelis, A., Two-layer model for photomodulated thermoreflectance of semiconductor wafers. *Journal of Applied Physics*, 1996, **80**, 1713–11725.
14. Chen, G. and Borca-Tasciuc, T., Photothermal pyrometry for temperature measurement. *ASME HTD*, 1996, **327**, 47–54.
15. Sze, S. M., *Physics of Semiconductor Devices*. Wiley, New York, 1981.
16. Rosencwaig, A., Thermal wave characterization and inspection of semiconductor materials and devices. In *Photoacoustic and Thermal Wave Phenomena in Semiconductors*, ed. A. Mandelis. North Holland, New York, 1987, pp. 97–135.
17. Sturm, J. C. and Reaves, C. M., Silicon temperature measurement by infrared absorption: fundamental processes and doping effects. *IEEE Transactions on Electron Devices*, 1992, **39**, 81–88.
18. Sato, T., Spectral emissivity of silicon. *Jap. J. Appl. Phys.*, 1967, **6**, 339–347.